Randomized Trial

Ultrasound- and Fluoroscopy-Guided Curved Needle Lumbar Sympathetic Radiofrequency Ablation for Diabetic Peripheral Neuropathy Pain: A Randomized Trial

Meirong Wang, MD[1], Jing Li, MD[2], Chuiliang Liu, PhD[1], Xiao Wu, MD[1], Jingquan Wang, MB[1], and Yaya Li, MB[1]

From: [1]Foshan Fosun Chancheng Hospital, Foshan, China; [2]Foshan Clinical Medical School of Guangzhou University of Chinese Medicine, Foshan, China

Address Correspondence:
Chuiliang Liu, PhD
Foshan Fosun Chancheng HospitalNo.3 Shiwan Sanyou South Road, Chancheng District, Foshan City, Foshan, Guangdong 528031, China
E-mail: lcl1204@aliyun.com

Disclaimer: Meirong Wang and Jing Li are co-first authors. The present study was supported by Medical Science Technology Research Of Foshan (222000100381 2); Foshan Science and Technology Innovation Project (Medical Science and Technology Innovation Platform of Construction Project) (FSoAA-KJ218-1301-0041).

Conflict of interest: Each author certifies that he or she, or a member of his or her immediate family, has no commercial association (i.e., consultancies, stock ownership, equity interest, patent/licensing arrangements, etc.) that might pose a conflict of interest in connection with the submitted article.

Article received: 09-25-2025
Revised article received: 04-03-2026
Accepted for publication: 04-16-2026

Free full article: www.painphysicianjournal.com

Background: Lumbar sympathetic ganglion radiofrequency ablation (LSGRF) is an effective pain relief technique for patients with diabetic peripheral neuropathic pain (DPNP). Fluoroscopy, when combined with ultrasound, can guide the needle tip to locate the lumbar sympathetic ganglion (LSG) accurately, but the vertebrae pose an obstruction.

Objectives: The purpose of this study is to compare the technical efficacy and clinical outcomes between curved-needle and straight-needle techniques for LSGRF in DPNP patients.

Study Design: A prospective, randomized design.

Setting: The study was carried out in the anesthesiology department of Foshan Fosun Chancheng Hospital, Foshan, China.

Methods: This study included 60 DPNP patients aged 18 to 80 years, with ASA grade II to III and BMI 18 to 30 kg/m^2, who underwent combinations of LSGRF and anhydrous ethanol under ultrasound and fluoroscopy guidance. The patients were divided randomly into the curved-needle group (Group C, n = 30) and the straight-needle group (Group S, n = 30). The primary endpoint was the duration of the procedure. Secondary outcomes included ablation success rate, fluoroscopic imaging time, number of needle redirections, frequency of needle-bone contacts, serial pain scores on the visual analog scale (VAS), and surgical complications.

Results: Group C demonstrated statistically significant advantages in procedural efficiency, including shorter operation time (10.6 ± 3.1 min vs. 15.2 ± 2.3 min, $P < 0.001$), fewer needle redirections (0.5 vs. 4.5, $P < 0.001$), and reduced bone contacts (1.0 vs. 4.0, $P < 0.001$), over Group S. While the ablation success rate was numerically higher in Group C (96.7% vs 90.0%), this difference did not reach statistical significance ($P = 0.611$). Both groups showed a significant reduction in VAS scores from their preoperative counterparts at all postoperative assessment time points ($P < 0.05$), but there was no significant difference in VAS scores between the groups. The complication rate was lower in Group C (3.33% vs. 13.33%, $P = 0.357$), but that result had no statistical significance.

Limitations: The analgesic effect of LSGRF and the temperature of the affected limb were evaluated based only on short-term outcomes.

Conclusions: Compared to the traditional straight needle, the curved needle can reduce the operation time and the number of needle redirections in LSGRF for treating DPNP. Satisfaction of both patients and anesthesiologists also increased when using the curved needle. However, no statistically significant differences were observed between the 2 types of needles in terms of success rate or post-procedural analgesic efficacy.

Key words: Diabetic peripheral neuropathic pain, lumbar sympathetic ganglion radiofrequency ablation, ultrasound, curved needle, anhydrous ethanol

Pain Physician 2026: 29:E645-E653

Diabetic peripheral neuropathic pain (DPNP) is one of the common complications experienced by diabetic patients, with a prevalence as high as 26% (1). The condition is characterized primarily by symmetric numbness, abnormal pain sensation, and hypersensitivity that progress from the distal to the proximal limbs, impairing patients' quality of life severely. At present, DPNP is mostly treated conservatively, with medication. However, in recent years, interventional treatments such as spinal cord stimulation, lumbar sympathetic ganglion neurolysis (LSGN), and lumbar sympathetic ganglion radiofrequency ablation (LSGRF) have played an important role in managing refractory DPNP (2). The lumbar sympathetic ganglia (LSG) are involved in the transduction and modulation of pain signals. Blocking sympathetic nerves can reduce ectopic discharges, thereby decreasing sensitization and excitation of primary sensory neurons (3,4), while also improving local blood supply and promoting the clearance of pain-producing substances and inflammatory mediators (5,6). The LSG are located deeply at the anterolateral aspect of the lumbar vertebral bodies and the anterior part of the psoas major muscle, adjacent to the kidneys and ureters. The L2 sympathetic ganglion is often located from the lower third of the second lumbar vertebra to the upper third of the third lumbar vertebra (7-9), a relatively fixed position. To avoid damage to blood vessels and organs, certain requirements for the puncture angle and depth are necessary when performing LSGRF.

How can the success rate of LSGRF be improved and puncture complications reduced? In the past, lumbar sympathetic ganglion block was typically performed using blind techniques, fluoroscopy, or CT guidance. Bedside ultrasound guidance clearly displays the needle trajectory and important surrounding structures such as muscles, nerves, and blood vessels and enables real-time observation of drug diffusion (10). However, ultrasound has difficulty visualizing deeper structures, whereas fluoroscopy has certain advantages in locating the needle tip. Combining ultrasound and fluoroscopy can improve puncture safety and positioning accuracy. Additionally, the success rate of puncture can be increased and the risk of repeated punctures reduced by changing the puncture path. Previously, we used straight needles for puncture. During LSGRF, the needle-tip target is located at the posterior part of the anterior edge of the vertebral body. The vertebral body blocks the path from the puncture point to the LSG. The needle must contact the vertebral body during puncture, and the straight needle must be withdrawn to the subcutaneous tissue to adjust the puncture path, which increases puncture-related injury. Based on anatomical relationships, we developed a curved-needle technique (Fig. 1) that effectively controlled and adjusted the needle-tip position, allowing for faster arrival at the target (Fig. 2). The primary objective of this study was to compare the puncture operation time between curved and straight needles when used in combined bedside ultrasound– and fluoroscopy-guided LSGRF as a treatment for DPNP. Secondary indicators included evaluating the success rate, fluoroscopic imaging time, number of needle redirections, frequency of needle-bone contacts, (VAS) pain scores on the serial visual analog scale, and surgical complications.

Methods

Inclusion Criteria and Exclusion Criteria

This study selected 60 patients with DPNP who had been unresponsive to conservative treatment for more than 6 months and undergone unilateral LSGRF under ultrasound guidance from May 2022 to February 2025. All patients met the diagnostic criteria issued by the American Diabetes Association (ADA), were aged 18-80 years, classified as ASA class II–III, and had a BMI of 18–30 kg/m². This study was approved by the institutional review board of Foshan Fosun Chancheng Hospital (ethical approval number: CYIRB-LCYJ-20220020-PJ-20220425), and the study was registered in the Chinese Clinical Trial Registry (ChiCTR2500100091). All patients participating in the study were informed of the risks and complications preoperatively and signed informed consent forms. The exclusion criteria were as follows: (1) severe heart, lung, liver, kidney, or other diseases; (2) severe diabetic complications, such as diabetic renal failure, diabetic heart disease, etc.; (3) skin ulceration, redness, swelling, or inflammatory infection at the puncture site; (4) disordered coagulation parameters; (5) history of lumbar laminectomy with internal fixation or severe anatomical variations, such as scoliosis, tumors, etc.; (6) history of chemical or thermal lumbar sympathetic neurolysis; (7) pregnancy; (8) allergy to local anesthetics, anhydrous ethanol, or iohexol injections; (9) mental illness or impaired consciousness that prevented cooperation with treatment.

The researchers who did not participate in the surgical operation divided the patients into 2 groups (n = 30), using the random number method: the curved-

needle group (Group C) and the straight-needle group (Group S). Group allocation was concealed in a sealed opaque envelope that was not opened until the last practical moment.

Surgical Procedure

After entering the operating room, patients were monitored noninvasively for blood pressure, heart rate, and pulse oxygen saturation. The temperature of both feet was monitored (with the soles selected as the measurement points). Each patient was then assisted into a lateral decubitus position with the affected side up. A thin pillow was placed under the waist, and restraint belts were used to secure the upper abdomen and lower limbs. After routine sterile disinfection, sterile surgical drapes were applied.

In Group C, the puncture needle (radiofrequency thermocoagulation electrode cannula curved needle, specification: 20G×150×5, model 240104 [Stryker Spine]) was pre-bent using a standard protractor, and the puncture needle was standardized to achieve the same curvature angle. The needle was bent approximately one cm from the tip, with a curvature of about 10 degrees (external angle). The outer arc of the curvature faced the bevel opening of the needle tip (Fig. 1). Group S used the same puncture needle as Group C but without pre-bending. All patients underwent ultrasound guidance using a low-frequency convex array probe (2-5 MHz) for paramedian sagittal scanning to locate the L2 transverse process. The ultrasound probe was then rotated 90 degrees, placed perpendicular to the spine, moved ventrolaterally, and placed at the posterior axillary line for transverse scanning. Clear "shamrock" images were obtained on ultrasound (11), formed by the quadratus lumborum superiorly, the erector spinae muscle posteriorly, and the psoas major anteriorly surrounding the L2 transverse process. The relatively complete shadow of the L2 vertebral body and the anterior inferior vena cava and abdominal aorta could be seen medial to the psoas major. The puncture point was at the lower third

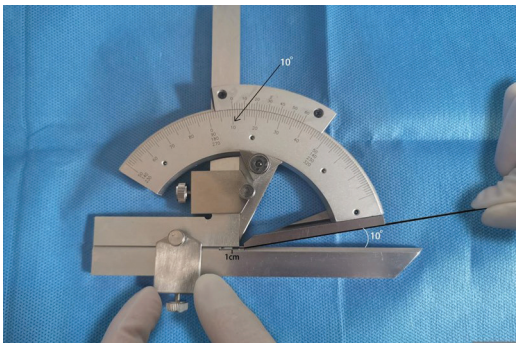


Fig. 1. *Customized curved needle. The radiofrequency thermocoagulation electrode cannula was pre-bent using a standard protractor. The needle was bent approximately 1 cm from the tip, with a curvature of about 10 degrees (external angle). The outer arc of the curvature faces the bevel opening of the needle tip.*

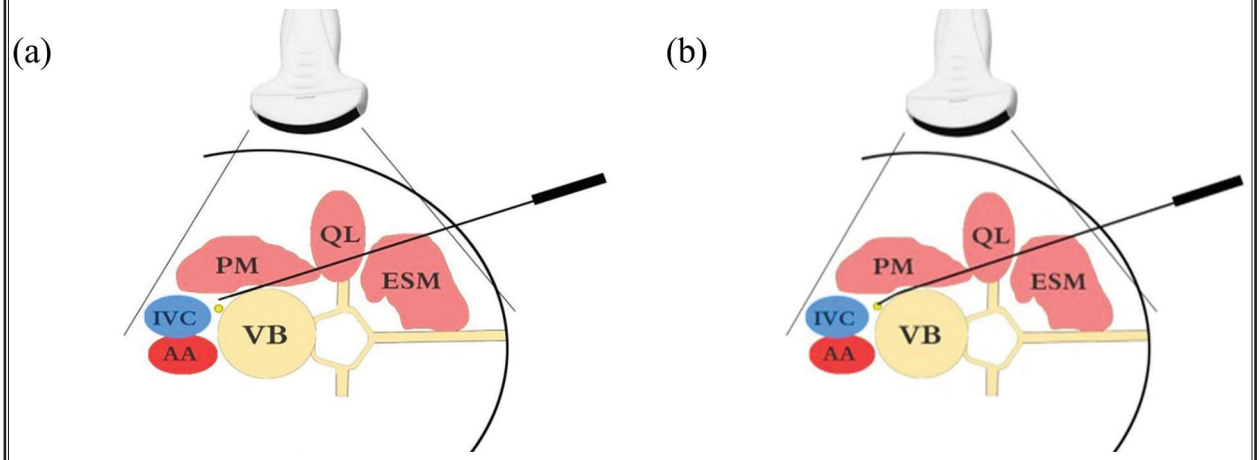


Fig. 2. *Schematic diagram of lumbar sympathetic ganglion radiofrequency ablation guided by straight needle (a) and curved needle (b).*
PM: psoas major; QL: quadratus lumborum; ESM: erector spinae muscle; IVC: inferior vena cava; AA: abdominal aorta

of the L2 vertebral body or the upper two-thirds of L3 (12), 6-8 cm beside the vertebral body. Before needle insertion, one mL of a 2% lidocaine hydrochloride injection was administered subcutaneously for local infiltration anesthesia. Under real-time ultrasound guidance, when the needle tip passed through the anterior fascia of the psoas major and reached the target (Fig. 3), fluoroscopy was used to confirm that the needle tip had reached the target (Fig. 4). Following negative aspiration for blood or cerebrospinal fluid, which confirmed that the needle tip was neither intravascular nor intramuscular, 3 mL of contrast agent (300 mgI/mL, 20 mL, batch No. 14787503) was injected. Fluoroscopy confirmed that the contrast agent diffused to the anterior aspect of the vertebral body wrapped by the anterior psoas major and the anterolateral vertebral body, with no adverse reactions or vascular escape. Radiofrequency electrode testing was performed: a sensory nerve stimulation test at 0.3-0.5 V and 50 Hz frequency, with no pain, soreness, or abnormal sensation reported by the patient. Next came a motor nerve stimulation test at 2 Hz and 0.3-0.5 V. The absence of muscle twitching in the lower back or lower limbs indicated successful testing. After one mL of 2% lidocaine was injected, radiofrequency ablation was performed for neurolysis. The ablation temperature started at 60 °C and was increased by 10°C every minute until reaching 90°C, for a total of 4 minutes. After ablation, 3 mL of anhydrous ethanol was injected before the puncture needle was withdrawn. Thirty minutes later, both groups underwent ultrasound again so the puncture site could be examined for injury and abnormal diffusion of the drug solution. The puncture procedure was performed by an anesthesiologist who had had more than 100 successful puncture experiences, assisted by a nurse for fluoroscopy operations.

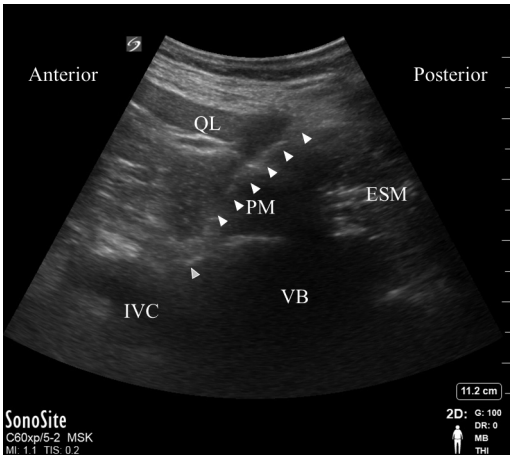


Fig. 3. *Transverse sonographic view of lumbar sympathetic ganglion radiofrequency ablation using a curved needle. The yellow arrow indicating the curved needle tip and the white arrow indicating the needle shaft.*
PM: psoas major; QL: quadratus lumborum; ESM: erector spinae muscle; IVC: inferior vena cava

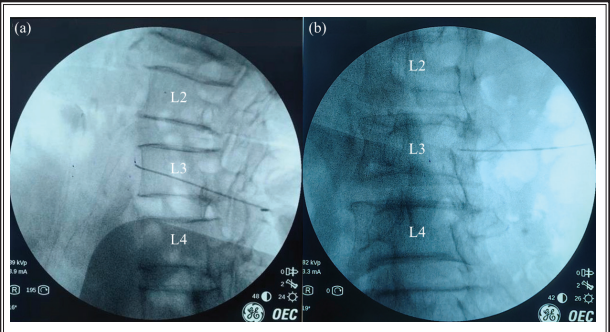


Fig. 4. *A lateral (a) and Anteroposterior (b) fluoroscopic view demonstrating a lumbar sympathetic radiofrequency ablation using a curved needle.*

Outcomes

The primary indicator of this study was the puncture operation time of LSGRF with straight and curved needles. Secondary indicators included the success rate of ablation, imaging time for both groups, time to plantar temperature increase by ≥ 2 °C, number of needle-bone contacts, number of needle redirections, treatment effects of both groups, and visual analog scale (VAS) scores before surgery and 30 minutes, one day, 3 days, 7 days, and one month after surgery. Puncture operation time was defined as the moment the needle touched the skin until the needle was withdrawn. The success rate of ablation was recorded in real time within 30 minutes before and after drug administration by measuring the rise in plantar skin temperature, with a temperature increase of 2°C as the criterion for successful ablation (13,14). Imaging time was defined as starting with the needle's contact with the skin and ending with the confirmation of good contrast diffusion at the anterolateral aspect of the vertebral body under fluoroscopy. Time to plantar temperature increase by ≥ 2 °C was defined as the time from procedure completion until plantar temperature increased by ≥ 2°C. The number of needle-bone contacts was the number of contacts between the needle and bone. The number of

needle redirections was defined as withdrawal of ≥ 2 cm, and re-advancement after the first needle insertion counted as one adjustment. VAS score ranged from 0 to 10, with 0 being no pain and 10 being the most severe pain. At 7 days and one month after treatment, the procedure's efficacy was evaluated based on pain scores and categorized into 4 grades: complete remission (CR), partial remission (PR), mild remission (MR), and no response (NR). The total remission rate was analyzed using the following formula: total remission rate (%) = [(CR + PR + MR)/n] × 100%. Surgery-related complications, such as infection, hematoma, vascular embolism, hypotension, organ injury, low back pain, nausea, vomiting, dizziness, and sensory and motor dysfunction related to genitofemoral nerve block or lumbar plexus block, were observed. The researchers responsible for postoperative pain assessment, follow-up, data collection, and analysis were unaware of the treatment group allocation.

Statistical Analysis

An a priori sample size calculation based on the primary outcome of procedure duration was performed using PASS 2021 (NCSS LLC). The pre-experiment data showed that the average difference in operation time between the 2 groups was 3.6 minutes, the common standard deviation was 3.8 minutes, and the resulting effect size (Cohen's d) was 0.95. With a significance level (α) of 0.05 for a 2-sided test and a power (1-β) of 90%, an independent samples t-test calculation indicated that a minimum of 27 patients per group was required. To account for a potential 10% dropout rate, we planned to enroll 30 patients in each group, resulting in a total sample size of 60 patients for this study.

Statistical processing was performed using IBM SPSS Statistics 24.0 (IBM Corporation). The normality of data was evaluated using the Kolmogorov-Smirnov test. Normally distributed measurement data were expressed as mean ± standard deviation ($\bar{x} \pm s$). Intergroup comparisons were performed using an independent samples t-test, and intragroup comparisons were performed using a paired t-test. Non-normally distributed measurement data were represented by median (M) and interquartile range (IQR). Repeated measures VAS scores were compared between groups by way of the Friedman test or Bonferroni correction. Count data were expressed as a composition ratio and analyzed using the χ^2 test. Rank data were compared using the rank-sum test. $P < 0.05$ was considered statistically significant.

Results

Demographic Data

We assessed the eligibility of 63 patients from May 2022 to February 2025. One patient was excluded due to a history of lumbar laminectomy with internal fixation, and 2 patients were excluded due to severe diabetic complications. Finally, 60 patients underwent LSGN (Fig. 4). Between the 2 groups, there were no statistically significant differences in preoperative baseline characteristics such as gender, age, BMI, ASA classification, surgical side, and preoperative VAS scores ($P > 0.05$, Table 1).

Operation-Related Data

The operation time (10.6 ± 3.1 vs. 15.2 ± 2.3 minutes, $P < 0.001$) and imaging time (5.8 ± 1.6 vs. 8.7 ± 2.0 minutes, $P < 0.001$) in Group C were significantly shorter than they were in Group S (Table 2). Group C required fewer needle-bone contacts [1.0 (0.0-1.0) vs. 4.0 (3.0-5.0), $P < 0.001$] and needle redirections [0.5 (0.0-1.0) vs. 4.5 (3.5-5.5), $P < 0.001$] to reach the target. The pre-postoperative foot temperature difference was higher in Group C (2.7 ± 0.5 vs. 2.4 ± 0.7°C, $P = 0.014$). The success rate of LSGRF was higher in Group C (96.7% vs. 90.0%, $P = 0.611$), but this difference was not statistically significant. Anesthesiologist and patient satisfaction were higher in Group C than in Group S ($P < 0.01$, Table 2).

Compared to the preoperative values, postoperative VAS scores decreased significantly in both groups. The 2 groups' comparative VAS scores before treatment and 30 minutes after treatment were (7.3 ± 1.3 vs. 7.5 ± 1.2, $P = 0.667$) and (1.9 ± 1.1 vs. 2.1 ± 1.3, $P = 0.652$), respectively. There were no statistically significant intergroup differences in VAS scores at different time points after surgery, but intragroup comparisons showed statistically significant differences ($P < 0.05$) (Table 3).

Although the proportion of CR was slightly higher in Group C (7 days postoperatively: 20.0% vs. 3.3%; one month postoperatively: 36.7% vs. 13.3%), these differences did not reach statistical significance. The total remission rate at 7 days and one month postoperatively was higher in Group C (96.67 vs. 90.00, $P = 0.067$; 93.33 vs. 90.00, $P = 0.330$), but the differences were not statistically significant. Comparisons of CR, PR, and MR between the 2 groups also showed no statistical significance ($P > 0.01$, Table 4).

In Group S, 2 patients developed small hematomas around the puncture sites, which showed significant

absorption and improvement upon reexamination after 7 days. One patient developed medically controllable hypotension, and another patient reported low back pain. In Group C, one patient reported low back pain. Overall, the complication rates in Group S and Group C were 13.33% and 3.33% respectively (P = 0.357). No patients showed any urinary, ejaculatory, or bowel dysfunction, or other serious complications.

Discussion

The pathogenesis of DPNP is complex. Some patients' refractory pain cannot be relieved by medication, and various physical therapies have been applied in such cases. Radiofrequency therapy, which has been used widely for sympathetically maintained pain that proves refractory to conservative treatment, is superior to other interventional techniques such as nerve blocks and chemical neurolysis (15,16). Interventional treatments such as LSGN and LSGRF are used widely to diagnose and treat such arterial occlusive diseases as ischemic rest pain, complex regional pain syndrome, and thromboangiitis obliterans. These treatments are also used for managing phantom limb pain, erythromelalgia, hyperhidrosis, and postherpetic neuralgia, due to the techniques' advantages, like precise destruction area, minimal damage, and long-lasting efficacy (17,18). The "sympathectomy effect" and sympathetic-sensory coupling effect are mechanisms by which lumbar sympathetic block can treat DPNP. Blocking sympathetic nerves can dilate blood vessels in the body, improve local blood supply, increase collateral circulation, improve lower limb tissue perfusion, reduce inflammatory response, decrease plasma endothelin (ET) release, and promote the elimination of pain-producing substances (19). When peripheral nerves are damaged, local inflammation promotes spontaneous activity, activates surrounding glial cells, and induces abnormal sprouting of LSG toward sensory neurons forming "basket"-like structures, creating sympathetic-sensory coupling (in which those "basket"-like structures may be formed around certain sensory neurons). This process can occur in areas of nerve injury and tissue inflammation, undamaged afferent nerve fibers, and dorsal root ganglia related to the injury areas (5). The sprouting tissue not only has highly localized excitability (20) but can also release epinephrine and norepinephrine (21), activating upregulated adrenergic receptors in the sensory neuronal cell membrane. The epinephrine and norepinephrine then make these receptors abnormally sensitive to excitation from postganglionic sympathetic fibers, activating neurons repeatedly and promoting a significant increase in ectopic discharges, which leads to sensitization of primary neurons and thus causes neuropathic pain and hyperalgesia (22-25). LSG ablation can block this pain conduction pathway, reduce sympathetic sprouting in the dorsal root ganglion, and decrease inflammatory mediators in patient plasma such as β-endorphin, norepinephrine, serotonin, and substance P, thereby alleviating pain (6). When LSGN is performed, the needle tip must be positioned accurately at the lumbar sympathetic trunk without diffusion into the lumbar muscle fascia and psoas major muscle. The lumbar muscle fascia contains the genitofemoral nerve or the contralateral sympathetic trunk. Diffusion of anhydrous ethanol can damage the sciatic nerve and even cause permanent injury to the lateral femoral cutaneous nerve (15,26). Fluoroscopy can locate the needle tip accurately and is the main tool for precise positioning in LSGRF.

Cheng et al (27) described a case of good efficacy that occurred after a DPNP patient received multiple bilateral LSG blocks at the L3 level under fluoroscopic guidance over a 26-month period. The effects lasted 2-4 months after the blockade. A randomized clinical trial by Ding et al (28) showed that for DPNP patients, the total remission rates one year after CT-guided treatment with anhydrous ethanol alone or radiofrequency thermocoagulation alone reached 66.7% and 73.3%, respectively. Meanwhile, according to the same researchers, remission rates among patients who received a combination of anhydrous ethanol and radiofrequency reached 93.3% one year after the operation, a finding similar to the results of this study. However, fluoroscopy has disadvantages, such as inconvenient operation, long imaging time, and radiation. The success rate of LSGN under fluoroscopy is about 67% (29-31). Ultrasound guidance allows real-time visualization of the needle tip, is convenient to operate, and has lower radiation exposure (32), but the technique's ability to image deep tissues is weak. The display rate for the key operative site, the psoas major muscle, is only 70%, the success rate of LSGB is only 65% (32), and the clinician performing the procedure cannot avoid the risk of intravenous injection. Using both ultrasound and fluoroscopy to guide the operation combines real-time guidance with precise positioning. Recent studies (33) have confirmed the feasibility of this method by performing LSGB at the L3 level between the kidney and lower adjacent vertebra via a shorter out-of-plane trajectory needle under

ultrasound and fluoroscopy. However, our team found in practice that the location of the LSG was difficult to reach directly, posing a risk of repeated puncture. Referring to the ultrasound localization method of Zhang et al (11), our team found that the path from the puncture port to the LSG was obstructed by the vertebral body, increasing the difficulty of puncture. Based on the anatomical structure, we invented a curved needle that could reach the target quickly. This study compared the effects of straight and curved needles for fluoroscopy- and ultrasound-guided LSGRF in patients with DPNP. The results indicate that using a curved needle for LSGRF provides a suitable puncture path and angle, keeping the needle path away from the vertebral body and reducing the number of needle redirections, quantity of needle-bone contacts, imaging time, and operation time compared to the straight-needle group, thus reducing puncture injury. Moreover, accurate needle tip positioning in Group C resulted in better short-term block effects, faster postoperative plantar temperature increase, and a higher pre-postoperative foot temperature difference, which might have been related to the more precise positioning and more complete nerve ablation seen with the curved needle. Patients and anesthesiologists were significantly more satisfied with the curved needle, and no serious complications occurred after either type of operation. The curved needle requires only a slight adjustment of the needle tip to adapt to different anatomical structures, improving operational efficiency, and has been used in various pain treatment methods (34-36). Although the ablation success rate and remission rate were higher with the curved needle, the difference was not statistically significant. VAS scores from 30 minutes to one month postoperatively decreased from their preoperative counterparts in both groups, but there was no intergroup difference, indicating that the 2 groups experienced equivalent analgesic efficacy. The high ablation success rates of 90% and 96.7% for straight and curved needles, respectively, provide clinical evidence that pain in diabetic neuropathy may be largely mediated sympathetically. Nonetheless, failures are still possible, which may be due to anatomical variability of the sympathetic trunk and ganglia in the lumbar region, degenerative spondylosis possibly causing displacement of LSG, or the fact that pain in some patients is not mediated entirely sympathetically. A potential concern with the curved needle is whether the slight bend requires additional insertion force, which may theoretically increase tissue trauma along the needle path. In our study, we did not observe any increase in intraprocedural complications or postoperative pain. Furthermore, immediate post-procedural ultrasound examination confirmed the absence of hematoma or tissue injury along the needle path. Nonetheless, we acknowledge that the effective local anesthetic and subsequent radiofrequency ablation may mask any transient discomfort from the needle passage. Future studies may consider objective measures of tissue trauma, such as MRI.

Limitations

The current study has several limitations. First, studies have shown that the median duration of LSGN is estimated to be 12 weeks (37) and can be up to 6 months (38), with possible recurrence. This issue may present itself because some nerve branches are not completely blocked or because compensation occurs through the neural network between the bilateral sympathetic trunks (15). Studies have shown that 19.5% of patients still show temperature changes in the contralateral foot after lumbar sympathetic block (39), confirming the complex interconnected neural network between bilateral sympathetic nerves. This study observed patients only up to one month after the procedure, so whether this method of radiofrequency thermocoagulation that uses a curved needle has a longer-term effect is unclear. Further multi-center and long-term follow-up studies are needed in the future to verify the long-term efficacy of the curved-needle technique. Second, studies have shown that in CRPS patients, there is no correlation between pain relief and body temperature increase after sympathetic block (40-42). Additionally, the study was limited by a single time-point observation, unable to infer a correlation between temperature increase and pain relief. The results only suggest that early temperature response may be a marker of successful LSGRF or an accompanying phenomenon of pain improvement. Multi-time point studies are needed to verify causal relationships. Although we recognize the limitations of the current study, the positive therapeutic results of the curved needle warrant further research.

Conclusions

In conclusion, compared with the straight-needle approach, the curved-needle technique combined with ultrasound and fluoroscopy guidance for LSGRF with ethanol can significantly reduce operative time and the

number of needle redirections, and is associated with higher satisfaction scores for both patients and anesthesiologists. However, no statistically significant differences were observed between the two types of needles regarding block success rate, analgesic effect, or postoperative complications. Given its accurate positioning and favorable safety profile, the curved-needle technique represents a viable alternative for LSGRF treatment.

Authors' Contributions

MRW and CLL helped with the conceptualization, design, and writing of this study. JL helped with the writing as well as data statistics, whereas XW aided in with data curation and statistics generation. JQW and YYL helped with the execution of the research. All authors read and approved the final version of the manuscript.

References

1. Zuidema X, de Galan B, Brouwer B, et al. 4. Painful diabetic polyneuropathy. *Pain Pract* 2024; 24:308-320.
2. Xu L, Sun Z, Casserly E, Nasr C, Cheng J, Xu J. Advances in interventional therapies for painful diabetic neuropathy: A systematic review. *Anesth Analg* 2022; 134:1215-1228.
3. Xing JL, Hu SJ, Jian Z, Duan JH. Subthreshold membrane potential oscillation mediates the excitatory effect of norepinephrine in chronically compressed dorsal root ganglion neurons in the rat. *Pain* 2003; 105:177-183.
4. Hu SJ, Yang HJ, Jian Z, et al. Adrenergic sensitivity of neurons with non-periodic firing activity in rat injured dorsal root ganglion. *Neuroscience* 2000; 101:689-698.
5. Zhang J, Deng Y, Geng M. Efficacy of the lumbar sympathetic ganglion block in lower limb pain and its application prospects during the perioperative period. *Ibrain* 2022; 8:442-452.
6. Sun H, He M, Pang J, Guo X, Huo Y, Ma J. Continuous lumbar sympathetic blockade enhances the effect of lumbar sympatholysis on refractory diabetic neuropathy: A randomized controlled trial. *Diabetes Ther* 2020; 11:2647-2655.
7. Hong JH, Kim AR, Lee MY, Kim YC, Oh MJ. A prospective evaluation of psoas muscle and intravascular injection in lumbar sympathetic ganglion block. *Anesth Analg* 2010; 111:802-807.
8. Gandhi KR, Verma VK, Chavan SK, Joshi SD, Joshi SS. The morphology of lumbar sympathetic trunk in humans: A cadaveric study. *Folia Morphol* 2013; 72:217-222.
9. Datta S, Pai U. Paradiscal extraforaminal technique for lumbar sympathetic block: Report of a proposed new technique utilizing a cadaver study. *Pain Physician* 2004; 7:53-57.
10. Hurdle MFB. Ultrasound-guided spinal procedures for pain. *Phys Med Rehabil Clin N Am* 2016; 27:673-686.
11. Zhang L, Qiu Y, Zhao W, Wang X. Ultrasound-guided lumbar sympathetic ganglion block: A visual teaching method. *Asian J Surg* 2022; 45:2382-2383.
12. Feigl GC, Dreu M, Ulz H, Breschan C, Maier C, Likar R. Susceptibility of the genitofemoral and lateral femoral cutaneous nerves to complications from lumbar sympathetic blocks: Is there a morphological reason? *Br J Anaesth* 2014; 112:1098-1104.
13. Greenstein D, Brown TF, Kester RC. Assessment of chemical lumbar sympathectomy in critical limb ischaemia using thermal imaging. *J Clin Monit Comput* 1994; 11:31-34.
14. Park SY, Nahm FS, Kim YC, Lee SC, Sim SE, Lee SJ. The cut-off rate of skin temperature change to confirm successful lumbar sympathetic block. *J Int Med Res* 2010; 38:266-275.
15. Zacharias NA, Karri J, Garcia C, Lachman LK, Abd-Elsayed A. Interventional radiofrequency treatment for the sympathetic nervous system: A review article. *Pain Ther* 2021; 10:115-141.
16. Xu P, Fan HR, Zhang EM, Zhang HN, Fei Y. Advances in the treatment of neuropathic pain by sympathetic regulation. *Curr Pain Headache Rep* 2024; 28:1167-1176.
17. Bovaira M, García-Vitoria C, Carrera A, et al. Human lumbar sympathetic blockade: An anatomical study to address potential block failure. *Clinical Anatomy* 2023; 36:360-371.
18. Liu B, Guo W, He Q, Wang S. Effect of lumbar sympathetic ganglion radiofrequency therapy combined with anhydrous ethanol on pain relief in patients with osteonecrosis of the femoral head. *Am J Transl Res* 2024; 16:4876-4884.
19. Keser-Pehlivan C, Kucukbingoz C, Pehlivan UA, Balli HT, Unlugenc H, Ozbek HT. Retrospective evaluation of the effect of lumbar sympathetic blockade on pain scores, Fontaine classification, and collateral perfusion status in patients with lower extremity peripheral arterial disease. *Medicina* 2024; 60:682.
20. Xie W, Strong JA, Mao J, Zhang JM. Highly localized interactions between sensory neurons and sprouting sympathetic fibers observed in a transgenic tyrosine hydroxylase reporter mouse. *Mol Pain* 2011; 7:53.
21. Wang C, Di A, Wu Y, et al. Sprouting sympathetic fibres release CXCL16 and norepinephrine to synergistically mediate sensory neuronal hyperexcitability in a rodent model of neuropathic pain. *Br J Anaesth* 2025; 134:804-816.
22. Chen SS, Zhang JM. Progress in sympathetically mediated pathological pain. *J Anesth Perioper Med* 2015; 2:216-225.
23. Pertin M, Allchorne AJ, Beggah AT, Woolf CJ, Decosterd I. Delayed sympathetic dependence in the spared nerve injury (SNI) model of neuropathic pain. *Mol Pain* 2007; 3:21.
24. Nascimento FP, Magnussen C, Yousefpour N, Ribeiro-da-Silva A. Sympathetic fibre sprouting in the skin contributes to pain-related behaviour in spared nerve injury and cuff models of neuropathic pain. *Mol Pain* 2015; 11:59.
25. Iwase T, Takebayashi T, Tanimoto K, et al. Sympathectomy attenuates excitability of dorsal root ganglion neurons and pain behaviour in a lumbar radiculopathy model. *Bone Joint Res* 2012; 1:198-204.

26. Pennekamp W, Krumova EK, Feigl GP, et al. Permanent lesion of the lateral femoral cutaneous nerve after low-volume ethanol 96% application on the lumbar sympathetic chain. *Pain Physician* 2013; 16:391-397.
27. Cheng J, Daftari A, Zhou L. Sympathetic blocks provided sustained pain relief in a patient with refractory painful diabetic neuropathy. *Case Rep Anesthesiol* 2012; 2012:1-5.
28. Ding Y, Yao P, Li H, Zhao R, Zhao G. Evaluation of combined radiofrequency and chemical blockade of multi-segmental lumbar sympathetic ganglia in painful diabetic peripheral neuropathy. *JPR* 2018; 11:1375-1382.
29. Schmid MR, Kissling RO, Curt A, Jaschko G, Hodler J. Sympathetic skin response: Monitoring of CT-guided lumbar sympathetic blocks. *Radiology* 2006; 241:595-602.
30. Gangi A, Dietemann JL, Mortazavi R, Pfleger D, Kauff C, Roy C. CT-guided interventional procedures for pain management in the lumbosacral spine. *Radiographics* 1998; 18:621-633.
31. Silbergleit R, Mehta BA, Sanders WP, Talati SJ. Imaging-guided injection techniques with fluoroscopy and CT for spinal pain management. *Radiographics* 2001; 21:927-939.
32. Ryu JH, Lee CS, Kim YC, Lee SC, Shankar H, Moon JY. Ultrasound-assisted versus fluoroscopic-guided lumbar sympathetic ganglion block: A prospective and randomized study. *Anesth Analg* 2018; 126:1362-1368.
33. Marada S, Punj J, Dhar A, et al. To assess the technical feasibility of ultrasound lumbar sympathetic block with electrical stimulation needle in out-of-plane needle orientation: A prospective interventional study. *Pain Medicine* 2022; 23:873-877.
34. Chen Y, Zhu Q, Huang B, et al. The value and application of personalized needle modification in percutaneous infrazygomatic radiofrequency in isolated maxillary nerve pain through the foramen rotundum. *Pain Physician* 2019; 22:377-387.
35. Wang M, Li J, Li Z, et al. Use of a curved needle to facilitate four-in-one nerve block performance after total knee arthroplasty in elderly patients: A randomized clinical trial. *Minerva Anestesiol* 2023; 89:289-297.
36. Noe C, van Hal M, Helm Ii S, Racz GB. Cervical nerve root block using a curved blunt needle and posterior approach. Pain Physician 2024; 27:161-168.
37. Choi EJ, Kim S, Lim D, et al. Effect duration of lumbar sympathetic ganglion neurolysis in patients with complex regional pain syndrome: A prospective observational study. *Sci Rep* 2024; 14:12693.
38. Choi EJ, Choi YM, Jang EJ, Kim JY, Kim TK, Kim KH. Neural ablation and regeneration in pain practice. *Korean J Pain* 2016; 29:3-11.
39. Cañada-Soriano M, Priego-Quesada JI, Bovaira M, et al. Quantitative analysis of real-time infrared thermography for the assessment of lumbar sympathetic blocks: A preliminary study. *Sensors (Basel)* 2021; 21:3573.
40. Kim J, Yun M, Han AH, et al. Thoracic sympathetic ganglion blocks: Real-world outcomes in 207 chronic pain patients. *Reg Anesth Pain Med* 2024; 49:528-535.
41. Dev S, Yoo Y, Lee HJ, Kim DH, Kim YC, Moon JY. Does temperature increase by sympathetic neurolysis improve pain in complex regional pain syndrome? A retrospective cohort study. *World Neurosurg* 2018; 109:e783-e791.
42. Samen CDK, Sutton OM, Rice AE, et al. Correlation between temperature rise after sympathetic block and pain relief in patients with complex regional pain syndrome. *Pain Medicine* 2022; 23:1679-1689.